X-ray absorption spectroscopy studies of Fe-doped misfit-layered $Ca_3Co_{4-x}Fe_xO_{9+\delta}$ (x=0, 0.05, 0.1, and 0.15)

Chia-Jyi Liu[a)]
Department of Physics, National Changhua University of Education, Changhua 500, Taiwan

Jeng-Lung Chen
Department of Physics, Tamkang University, Tamsui, 251 Taiwan

Li-Chen Huang and Zhi-Ru Lin
Department of Physics, National Changhua University of Education, Changhua 500, Taiwan

Ching-Lin Chang
Department of Physics, Tamkang University, Tamsui 251 Taiwan

(Received 30 April 2007; accepted 5 May 2007; published online 10 July 2007)

We have carried out O K- and Co $L_{2,3}$-edge x-ray absorption studies on misfit-layered oxides of polycrystalline $Ca_3Co_{4-x}Fe_xO_{9+\delta}$ (x=0,0.05,0.1,0.15). The analyses of integrated absorption intensity show that the number of Co 3d unoccupied states decreases upon partial substitution of Fe for Co, which correlates well the variation trend of the room-temperature resistivity with x. Nevertheless, the number of O 2p unoccupied states increases with x. Both Hall and thermopower measurements indicate that the majority carrier is of hole type for $Ca_3Co_{4-x}Fe_xO_{9+\delta}$. Therefore, the decrease of O 2p occupancy should be responsible for the increase of the hole carrier concentration upon partial substitution of Fe for Co. © *2007 American Institute of Physics*.
[DOI: 10.1063/1.2748722]

I. INTRODUCTION

The mistfit layered cobaltite $Ca_3Co_4O_{9+\delta}$ is particularly interesting due to its large thermopower and is therefore considered to be a good candidate for thermoelectric applications.[1–4] We have recently shown that thermoelectric characteristics of $Ca_3Co_4O_{9+\delta}$ can be improved by partial substitution of Fe for Co.[5] X-ray absorption near-edge structure (XANES) spectra can provide information of unoccupied states regarding the electronic structure of a material. Mizokawa *et al.* have recently studied the O K- and Co $L_{2,3}$-edges of $Ca_3Co_4O_9$.[6] Herein, we report the XANES studies of the Fe-doped cobaltites $Ca_3Co_{4-x}Fe_xO_{9+\delta}$ and find that the number of Co 3d unoccupied states decreases, while the number of O 2p unoccupied states increases upon partial substitution of Fe for Co.

II. EXPERIMENT

Polycrystalline cobaltites $Ca_3Co_{4-x}Fe_xO_{9+\delta}$ (x=0, 0.05, 0.1, and 0.15) were synthesized using conventional solid state reaction methods. All the x-ray diffraction (XRD) peaks of $Ca_3Co_{4-x}Fe_xO_{9+\delta}$ are indexable using superspace group of $X2/m(0b0)s0$. Room-temperature O K-, Co $L_{2,3}$-, and Fe $L_{2,3}$-edge XANES spectra were acquired at the beamline BL20A (HSGM), and Co K- and Fe K edge XANES spectra were acquired at the beamline BL17C (Wiggler-C) of the National Synchrotron Radiation Research Center (NSRRC), Hsinchu, Taiwan. O K-, Co K, and Fe K-edge XANES data were taken in a fluorescence mode, while $L_{2,3}$-edge XANES data were taken in a total electron yield mode.

III. RESULTS AND DISCUSSION

Figure 1 presents the Co K-edge XANES spectra of $Ca_3Co_{4-x}Fe_xO_{9+\delta}$ as well as those of the reference materials (CoO and Co_2O_3). Features $A1$ and $B1$ are attributed, respectively, to quadrupole allowed transition from Co 1s core level to O 2p-Co 3d hybridized states and transition from Co

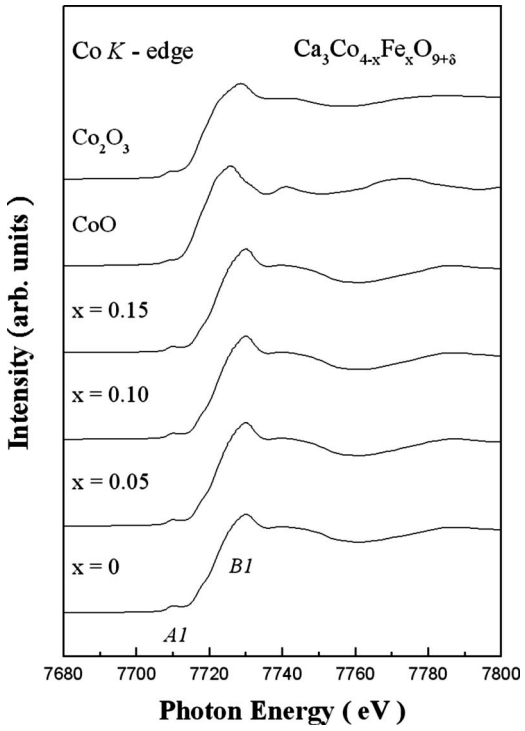

FIG. 1. Co K-edge XANES spectra of $Ca_3Co_{4-x}Fe_xO_{9+\delta}$ (x=0, 0.05, 0.10, and 0.15) and the reference oxides.

[a)]Electronic mail: liucj@cc.ncue.edu.tw

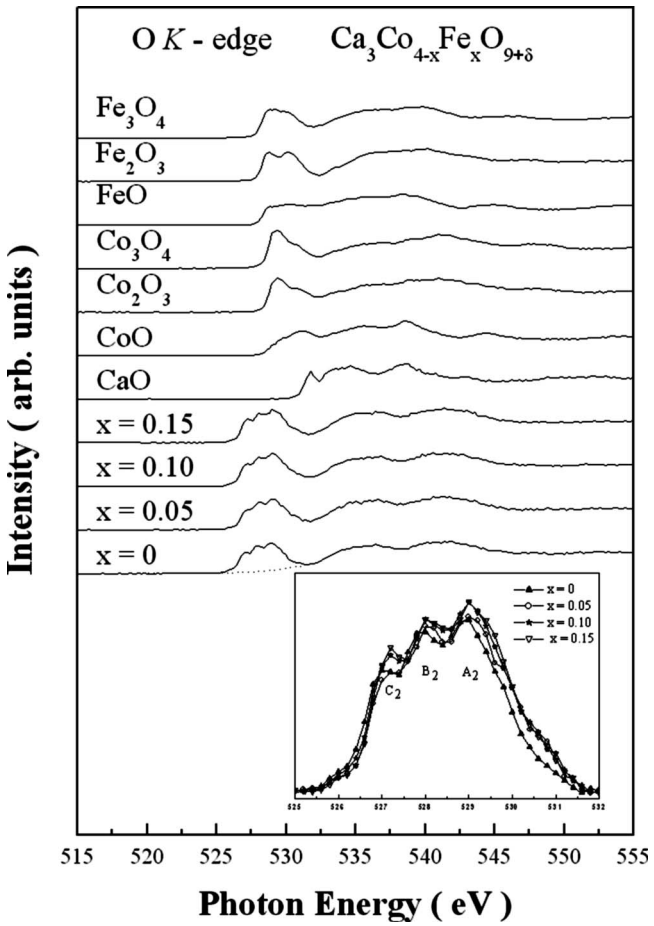

FIG. 2. O *K*-edge XANES spectra of $Ca_3Co_{4-x}Fe_xO_{9+\delta}$ (x=0, 0.05, 0.10, and 0.15) and the reference oxides. The inset shows the magnified preedge peaks after background subtraction using a best fitted Gaussian curve indicated by the dotted line.

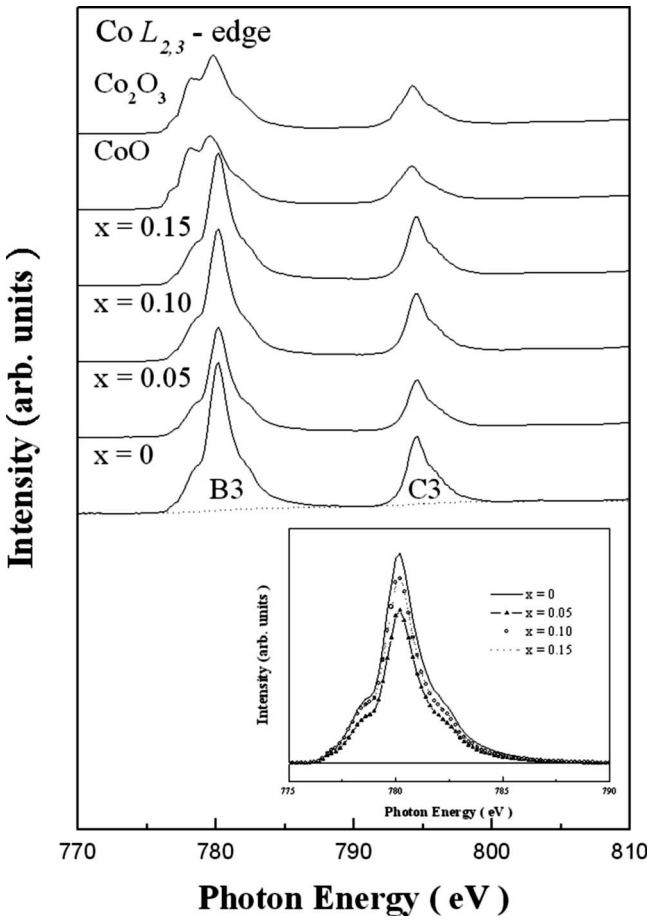

FIG. 3. Co $L_{2,3}$-edge XANES spectra of $Ca_3Co_{4-x}Fe_xO_{9+\delta}$ (x=0, 0.05, 0.10, and 0.15) and the reference oxides. The inset shows the magnified L_3-edge after background subtraction using an arctangent function indicated by the dotted line.

1*s* core level to unoccupied 4*p* states according to the dipole selection rule. There is no energy shift observed for the main absorption edge after energy calibration, indicating that the absorption energy is insensitive to the Fe doping. Figure 2 presents the O *K*-edge spectra of $Ca_3Co_{4-x}Fe_xO_{9+\delta}$ and the reference oxides (CaO, CoO, Co_2O_3, Co_3O_4, FeO, Fe_2O_3, and Fe_3O_4). The XANES spectra of $Ca_3Co_{4-x}Fe_xO_{9+\delta}$ are clearly different from those of the reference oxides. For pure ionic oxides, there would be no $1s \rightarrow 2p$ transition in the O *K*-edge spectra due to no unoccupied 2*p* states of O^{2-} ion. The electric-dipole-allowed $1s \rightarrow 2p$ transition comes from the presence of covalent mixing of the transition metal and oxygen states. Therefore, it can provide information on the charge state of oxygen and the Co–O bonding information. These preedge features are similar to those observed for $La_{2-x}Sr_xLi_{0.5}Co_{0.5}O_4$ and are attributed to the transition of O 1*s* electron to the unoccupied O 2*p*-Co 3*d* hybridized states between 525 and 532 eV.[7] There are two regions in the O *K*-edge spectra. The broader feature above 532 eV is assigned to oxygen *p* character hybridized with transition metal 4*s* and 4*p* states.[8] Feature *A*2 at 529 eV is associated with low-spin Co^{3+} and could be assigned to a $\underline{1s}(O)3d^7(Co)$ final state. Features *B*2 at 528 eV and *C*2 at 527 eV are associated with Co^{4+}, which has larger effective nuclear charge than Co^{3+} and thus causes the peak position to shift to lower energy.

Figure 3 presents the Co $L_{2,3}$-edge XANES spectra of $Ca_3Co_{4-x}Fe_xO_{9+\delta}$ and the reference materials (CoO and Co_2O_3). Features *B*3 (780 eV) and *C*3 (795 eV) are associated with the L_3- and L_2-edges due to electron transitions from their initial state of $2p_{3/2}$ and $2p_{1/2}$, respectively, to unoccupied 3*d* states hybridized with O 2*p* orbital.[9,10] The line shape of the Co $L_{2,3}$-edge XANES is similar to the atomic-multiplet calculations assuming the low-spin configurations (a t_{2g}^6 ground state for Co^{3+} ion and a t_{2g}^5 ground state for Co^{4+} ion).[11,12] These results are consistent with magnetization measurements. The Co^{+3} and Co^{+4} ions with a low-spin configuration have a theoretical effective magnetic moment of $0\mu_B$/Co and $1.73\mu_B$/Co, respectively. The Co^{+3} and Co^{+4} ions with a high-spin configuration have a theoretical effective magnetic moment of $4.89\mu_B$/Co and $5.91\mu_B$/Co, respectively. Figure 4 shows the plot of the magnetization as a function of temperature for x=0.05, which has a ratio of Co^{3+}/Co^{4+}=0.73/0.27. Table I shows the measured magnetic moments for $Ca_3Co_{4-x}Fe_xO_{9+\delta}$. The observed magnetic moment is close to the calculated values with both of the Co^{+3} and Co^{+4} ions having the low-spin configuration. It should be noted that the partial unoccupied O 2*p* states could contribute to the magnetic moments. The presence of mixed valence of Co^{3+} and Co^{4+} could enhance the hybridization between Co 3*d* and O 2*p* and in turn the charge transfer via double exchange mechanism.[9]

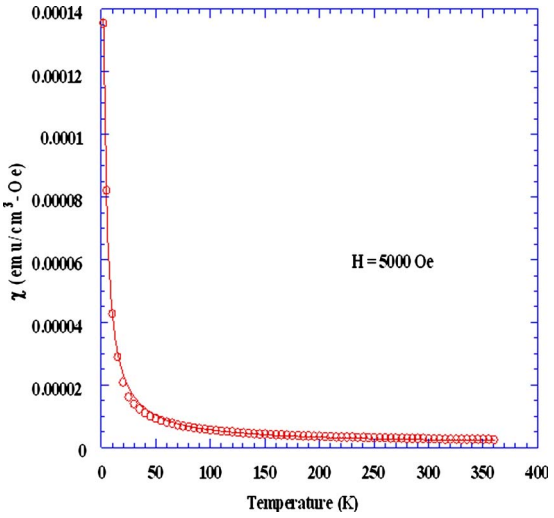

FIG. 4. (Color online) Plot of magnetic susceptibility vs T for $Ca_3Co_{3.95}Fe_{0.05}O_{9+\delta}$ in an applied field of 5000 Oe. The solid line is a fit to the Curie-Weiss law.

Figure 5 shows the integrated intensities of the Co L_3 and O K-edges and preedge features of the Fe K- and Co K-edges for $Ca_3Co_{4-x}Fe_xO_{9+\delta}$ (x=0, 0.05, 0.10, and 0.15). The intensity of O K-edge increases upon Fe doping, suggesting either an increase of the oxygen $2p$ holes induced by covalence or an increase of the oxygen content in the sample. However, the variation with Fe doping for the O K-edge intensity is rather small. Therefore, when considering the matrix-element effects, the O $2p$ unoccupied states seem to be insensitive to the Fe doping. Nevertheless, it should be noted that the oxygen content increases upon Fe doping according to the titration data. The number of unoccupied Co $3d$-O $2p$ hybridized states, obtained from the size of peak area of the L_3-edge, decreases upon Fe doping and the minimum occurs at x=0.05, where a resistivity minimum in the series of title materials also occurs. Furthermore, the Co K preedge intensity seems to decrease upon Fe doping even though the variation is rather small. The variation of room-temperature resistivity with x for $Ca_3Co_{4-x}Fe_xO_{9+\delta}$ seems to correlate well with the trend of variation of the size of peak area with x, as shown in the inset of Fig. 5. The more the Co $3d$ unoccupancy is, the higher the resistivity is. Since both thermopower and Hall measurements confirm the holes as the majority carriers for the title materials, this trend seems to be opposite to the variation of the carrier concentration

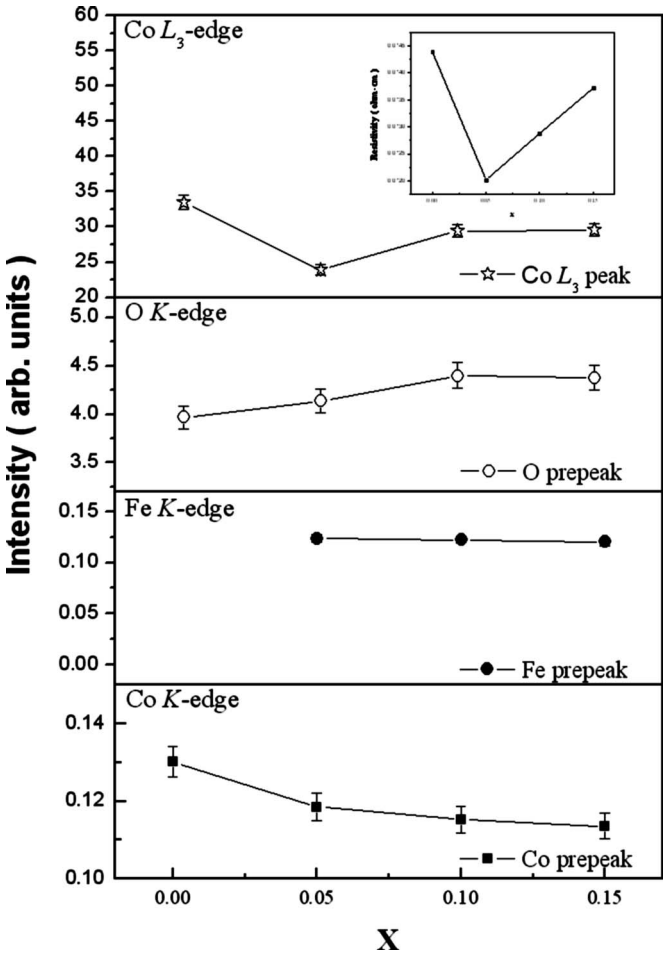

FIG. 5. Integrated intensities of the Co L_3- and O K-edges and preedge features of Fe K- and Co K-edges for $Ca_3Co_{4-x}Fe_xO_{9+\delta}$ (x=0, 0.05, 0.10, and 0.15). The intensity of Fe K-edge remains unchanged for all x. The inset is the variation of the room-temperature resistivity with x.

with x obtained by the Hall measurements with the highest carrier concentration of holes occurring at x=0.05 (Table I). Furthermore, the iodometric titration data (Table I) show that the variation of the average oxidation number v+ of $[CoO]^{v+}$ with x agrees well with that of the hole concentration from the Hall measurements. In light of the decrease of the Co $3d$ unoccupied states upon Fe doping, one may interpret that the increase of the oxygen $2p$ unoccupied states is responsible for the increase of the hole carrier concentration, which is closely associated with the oxygen content of the sample determined by the iodometric titration (Table I).

TABLE I. Effective magnetic moment of Co, carrier concentration, average oxidation number, and oxygen content of $Ca_3Co_{4-x}Fe_xO_{9+\delta}$ (x=0–0.1).

x	μ_{eff}[a] (μ_B/Co)	μ_{eff} (calc. μ_B/Co)	n (cm^{-3})	$[CoO]^{v+}$[b]	δ[b]	Co^{3+}/Co^{4+}
0	1.11	0.26	$+1.856\times10^{20}$	+1.15(1)	0.30(1)	0.85/0.15
0.05	0.38	0.47	$+2.762\times10^{20}$	+1.27(5)	0.54(9)	0.73/0.27
0.1	0.42	0.43	$+2.392\times10^{20}$	+1.25(1)	0.49(1)	0.75/0.25

[a]The observed effective magnetic moment is derived by fitting the magnetization vs T using the Curie-Weiss law. The slight variation of magnetic moment from calculated value might be due to the hybridization of the Co $3d$ with the O $2p$ states (Ref. 13).
[b]Both $[CoO]^{v+}$ and δ are determined by iodometric titration. Oxygen nonstoichiometry of $Ca_3Co_4O_{9+\delta}$ has been confirmed by thermogravimetry (Ref. 14).

IV. CONCLUSIONS

In summary, O *K*- and Co $L_{2,3}$-edge XANES spectra have been obtained on $Ca_3Co_{4-x}Fe_xO_{9+\delta}$. The variation of the number of Co 3*d* unoccupied states correlates well the variation of room-temperature resistivity with *x* for $Ca_3Co_{4-x}Fe_xO_{9+\delta}$. Both Hall and thermopower measurements indicate that the majority carrier of $Ca_3Co_{4-x}Fe_xO_{9+\delta}$ is of *p* type. Therefore, the increase of the number of O 2*p* unoccupied states should be responsible for the increase of the hole carrier concentration upon partial substitution of Fe for Co.

ACKNOWLEDGMENTS

This work was supported by the National Science Council of Taiwan, R.O.C. under Grant Nos. NSC 95-2112-M-018-006-MY3 (C.J.L.) and NSC 95-2112-M-032-008 (C.L.C.).

[1] S. Li, R. Funahashi, I. Matsubara, K. Ueno, and H. Yamada, J. Mater. Chem. **9**, 1659 (1999).
[2] A. C. Masset, C. Michel, A. Maignan, M. Hervieu, O. Toulemonde, F. Studer, B. Raveau, and J. Hejtmanek, Phys. Rev. B **62**, 166 (2000).
[3] Y. Miyazaki, M. Onoda, T. Oku, M. Kikuchi, Y. Ishii, Y. Ono, Y. Morii, and T. Kajitani, J. Phys. Soc. Jpn. **71**, 491 (2002).
[4] G. Xu, R. G. Funahashi, M. Shikano, I. Matsubara, and Y. Zhou, Appl. Phys. Lett. **80**, 3760 (2002).
[5] C.-J. Liu, L.-C. Huang, and J.-S. Wang, Appl. Phys. Lett. **89**, 204102 (2006).
[6] T. Mizokawa, L. H. Tjeng, H.-J. Lin, C. T. Chen, R. Kitawaki, I. Terasaki, S. Lambert, and C. Michel, Phys. Rev. B **71**, 193107 (2005).
[7] S. A. Warda, W. Massa, D. Reinen, Z. Hu, G. Kaindal, and F. M. F. de Groot, J. Solid State Chem. **146**, 79 (1999).
[8] F. M. F. de Groot, M. Grioni, J. C. Fuggle, J. Ghijsen, G. A. Sawatzky, and H. Petersen, Phys. Rev. B **40**, 5715 (1989).
[9] R. Asahi, J. Sugiyama, and T. Tani, Phys. Rev. B **66**, 155103 (2002).
[10] W.-S. Yoon, K.-B. Kim, M.-G. Kim, M.-K. Lee, H.-J. Shin, and J.-M. Lee, J. Electrochem. Soc. **149**, A1305 (2002).
[11] M. Abbate *et al.*, Phys. Rev. B **47**, 16124 (1993).
[12] R. H. Potze, G. A. Sawatzky, and M. Abbate, Phys. Rev. B **51**, 11501 (1995).
[13] M. A. Korotin, S. Yu, Ezhov, I. V. Solovyev, and V. I. Anisimov, Phys. Rev. B **54**, 5309 (1996).
[14] J.-I. Shimoyama, S. Horii, K. Ozachit, M. Sano, and K. Kishio, Jpn. J. Appl. Phys., Part 2 **42**, L194 (2003).